Chapter 3
Feed Forward Converter
and Pulse Width Modulator

Introduction

The Feed Forward Converter uses estimates of the motor parameters and the rotor position to generate 2-phase output voltage reference signals v_α and v_β. A software section of the Pulse Width Modulator then converts these voltage signals to pulse widths for a 2-phase motor. If a 3-phase motor is used, the pulse widths for the 2-phase motor are further converted to pulse widths for a 3-phase motor. The pulse widths are then converted to gate drive signals by the on-chip hardware section of the Pulse Width Modulator, which are sent out to the inverter gate drivers.

Feed Forward Converter

The Feed Forward Converter block generates the motor voltages from the applied *d* and *q* axes currents i'_d and i'_q for an applied rotor electrical angle θ'. The outputs of this block are the 2-phase applied motor voltage signals, v'_α and v'_β, for use by the Pulse Width Modulator. These outputs are generated using the motor equations linking i_d and i_q to v_α and v_β, which are derived as follows:

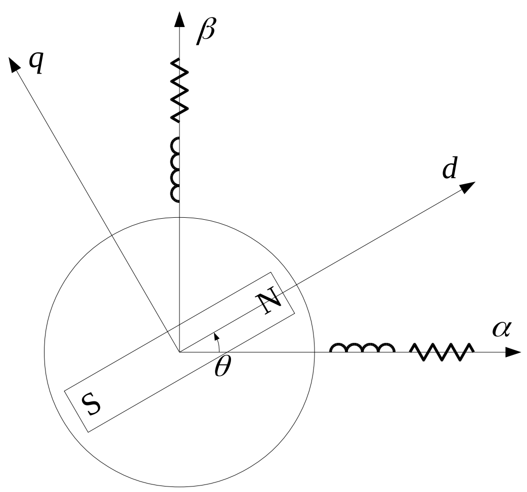

Figure 3.1. Diagram showing the fixed and rotating axes representations of the two-phase, two-pole equivalent PMSM.

Using the stationary $\alpha\beta$ axes shown in Figure 3.1, the motor voltages are found from the motor currents and rotor flux components by the equation:

$$\begin{bmatrix} v_\alpha \\ v_\beta \end{bmatrix} = \begin{bmatrix} R\,i_\alpha \\ R\,i_\beta \end{bmatrix} + \frac{d}{dt}\begin{bmatrix} L\,i_\alpha + \lambda_{r\alpha} \\ L\,i_\beta + \lambda_{r\beta} \end{bmatrix} \qquad (3.1)$$

where R and L are the stator resistance and inductance, and $\lambda_{r\alpha}$ and $\lambda_{r\beta}$ are the flux linkages in the α and β axes from the rotor. It is assumed the motor has no saliency and thus the stator inductances do not vary with the rotor angle.

Converting the stationary $\alpha\beta$ frame currents and flux linkages to the rotating dq frame shown in Figure 3.1 using the general conversion formula:

$$\begin{bmatrix} \alpha \\ \beta \end{bmatrix} = \begin{bmatrix} \cos\theta & -\sin\theta \\ \sin\theta & \cos\theta \end{bmatrix} \begin{bmatrix} d \\ q \end{bmatrix} \tag{3.2}$$

and assuming the rotor flux is aligned on the d axis, giving $\lambda_{rd} = \lambda_r$, the peak rotor flux linkage, and $\lambda_{rq} = 0$, the following equation is obtained:

$$\begin{bmatrix} v_\alpha \\ v_\beta \end{bmatrix} = \begin{bmatrix} \cos\theta & -\sin\theta \\ \sin\theta & \cos\theta \end{bmatrix} \begin{bmatrix} R\,i_d \\ R\,i_q \end{bmatrix} + \frac{d}{dt} \begin{bmatrix} \cos\theta & -\sin\theta \\ \sin\theta & \cos\theta \end{bmatrix} \begin{bmatrix} L\,i_d + \lambda_r \\ L\,i_q \end{bmatrix} \tag{3.3}$$

This is the equation implemented in the Feed Forward Converter.

Note that Equation 3.3 can be expanded further to the following familiar motor voltage equations in the dq frame:

$$\begin{bmatrix} v_d \\ v_q \end{bmatrix} = \begin{bmatrix} R+Lp & -\omega L \\ \omega L & R+Lp \end{bmatrix} \begin{bmatrix} i_d \\ i_q \end{bmatrix} + \omega\lambda_r \begin{bmatrix} 0 \\ 1 \end{bmatrix} \tag{3.4}$$

where p is used as the differential operator d/dt to improve clarity. Speed ω is $d\theta/dt$.

The expansion is most easily undertaken by putting:

$$\begin{bmatrix} v_\alpha \\ v_\beta \end{bmatrix} = \begin{bmatrix} \cos\theta & -\sin\theta \\ \sin\theta & \cos\theta \end{bmatrix} \begin{bmatrix} v_d \\ v_q \end{bmatrix} \tag{3.5}$$

followed by expanding the differentials and some careful algebraic manipulation.

The use of Equation 3.4 followed by conversion of v_d and v_q in the rotating frame to v_α and v_β in the stationary frame using Equation 3.5 is the basis of most field-oriented control implementations, but, as will be shown shortly, using the more primitive Equation 3.3 gives better results.

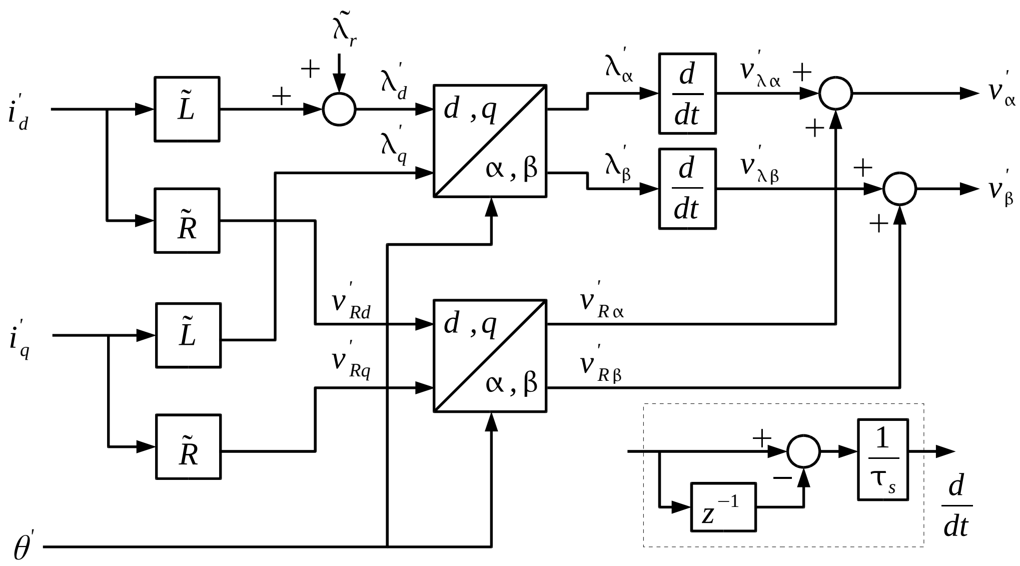

Figure 3.2. Implementation of Equation 3.3 in the Feed-Forward Converter.

A block diagram of the implementation of Equation 3.3 using estimated values of the motor parameters and applied values of the variables is shown in Figure 3.2. Variables v'_{Rd}, v'_{Rq}, $v'_{R\alpha}$ and $v'_{R\beta}$ are the calculated IR voltage drops in the *dq* and *αβ* axes. Variables λ'_d, λ'_q, λ'_α, λ'_β, $v'_{\lambda\alpha}$ and $v'_{\lambda\beta}$ reference intermediate calculated values.

As shown in the inset in the *z* domain, where z^{-1} is a one-sample period delay, the derivative is handled by subtracting the previous sample value of the flux from the present sample value, then scaling by the inverse of the sample period τ_s. The resulting output voltage values before adding IR voltage drops are given by:

$$
\begin{aligned}
v'_{\lambda\alpha} &= \frac{1}{t_s}\left(\lambda'_{\alpha(k)} - \lambda'_{\alpha(k-1)}\right) \\
v'_{\lambda\beta} &= \frac{1}{t_s}\left(\lambda'_{\beta(k)} - \lambda'_{\beta(k-1)}\right)
\end{aligned}
\tag{3.6}
$$

where the (*k*) and (*k*-1) subscripts refer to the present and previous sample values.

Ignoring the IR voltage drop contributions to the output voltage values v'_α and v'_β, making $v'_\alpha = v'_{\lambda\alpha}$ and $v'_\beta = v'_{\lambda\beta}$, and assuming the applied flux values λ'_α and λ'_β match the actual motor flux values, then v'_α and v'_β (which become the pulse width values after scaling) are related to the actual motor voltages v_α and v_β by the equations:

$$
\begin{aligned}
v'_\alpha &= \frac{1}{t_s}\int_{t_{k-1}}^{t_k} v_\alpha dt \\
v'_\beta &= \frac{1}{t_s}\int_{t_{k-1}}^{t_k} v_\beta dt
\end{aligned}
\tag{3.7}
$$

where t_k is the time at sample *k*, and t_{k-1} is the time at the previous sample *k*-1. As can be seen, each of the applied voltage values v'_α and v'_β is actually the average of each output voltage v_α and v_β over the sample interval t_{k-1} to t_k. This is a very important result as it yields much improved PWM accuracy.

The *dq* to αβ conversion block is implemented using sine and cosine look-up tables. The tables do not need to be very accurate because an error in one sample will carry over and be automatically corrected in the next sample.

A part of the feed-forward implementation scheme is the direct *dq* to αβ vector rotation of the estimated motor IR drop voltages. Since these added voltages compensate only for the motor resistance voltage drops, the look-up tables for the *dq* to αβ conversion also do not need to be very accurate.

The L/R time constant in the Feed Forward converter can cause excessively long settling times to load changes if it is too large. This occurs in very large motors, which have a very small winding resistance, and in stepper motors, which have a very large winding inductance. This is corrected by adding extra artificial resistance to the inverter outputs using feedback and increasing the estimated resistance $\tilde{R}$ to match the extra artificial resistance, reducing the L/R time constant to a suitable value. The selection of this extra resistance is described in a later chapter.

Advantages of Feed-Forward Conversion

The improved PWM accuracy obtained by using average voltage values as described in Equation 3.7 is illustrated in Figure 3.3. This shows the area of the pulse width generated by the traditional sampling of the actual α phase output voltage v_α rather than its average value. As can be seen, the area of the pulse width differs from the actual area under v_α, the amount depending on the double derivative of v_α. The improvements that can be obtained by using average voltage values are documented in reference [1].

Further reduction in waveform distortion could be obtained by using the next higher-order modulation scheme that chooses the pulse width in a sample interval so that the average of the average voltage is minimised. This scheme is called double integral modulation. An example of this higher-order scheme applied to cycloconverters can be found in reference [2].

The biggest problem of not using the average value of voltage for the pulse width generation process is that when the PWM carrier frequency is not an exact multiple of the output sine wave frequency, a low-frequency beating effect can occur, producing a low-frequency offset voltage, which in turn can produce large low-frequency torque modulation. This becomes worse as the ratio between the PWM carrier frequency and the output frequency reduces. The preferred limit to this ratio before the beating effect becomes serious is usually about 15:1 for a 3-phase motor with an absolute limit of about 10:1. If traditional inner current feedback loops are used instead of the feed forward converter described here, the feedback control of the currents greatly reduces the beating effect, but the delays in the PWM generation and in the current measurement limit the current loop bandwidth to an amount that again limits the carrier to output frequency ratio to greater than 10:1.

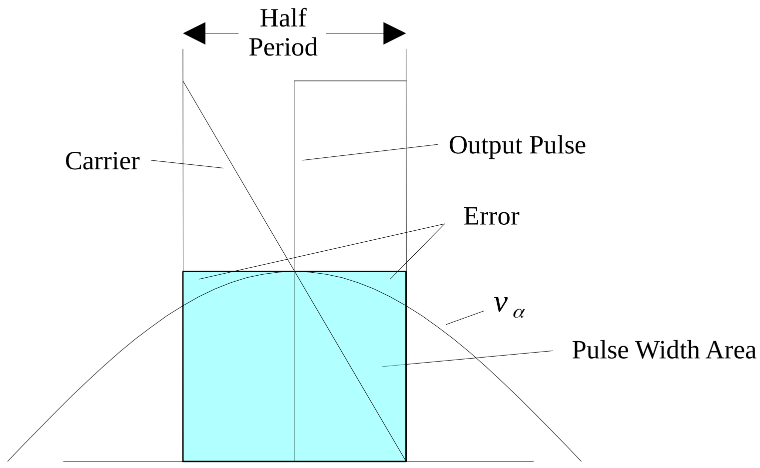

Figure 3.3. Illustration of error in output pulse width area.

Another advantage of using feed-forward current-to-voltage conversion instead of current feedback loops is that no extra voltage headroom is required on the output to ensure feedback stability. In most cases, the output can even be allowed to over-modulate without detrimental effects other than the higher current distortion.

Finally, a major advantage is that the Feed Forward Converter allows instantaneous control of the current vector applied to the motor windings in both amplitude and especially in position. If, for example, current is flowing in one motor coil and the applied angle θ' is changed by one coil pitch, the correct pulse widths will be applied to automatically move the current vector to the next coil. With traditional current feedback control, a change in angle does not result in the current vector moving. Instead, the resulting current vector position error is detected and eventually corrected by the current feedback loops.

Pulse Width Modulation

For a 2-phase motor, the pulse width modulator converts the voltage reference signals to the pulse widths required to drive the 2-phase inverter of Figure 2.2(a). Each phase is completely independent and is fed by a sinusoidal voltage reference signal, greatly simplifying the conversion process.

Each phase has two half-bridge inverter legs driving each of the two sides of the motor winding. The pulse width modulator treats each inverter leg independently, generating the pulse widths for each one separately. The resulting PWM waveform for the α phase and how it is generated is shown in Figure 3.4.

For the *A*-side inverter leg, the v'_α reference is compared directly to the triangular carrier waveform to generate the PWM pattern. As shown in the figure, the v'_α reference is updated at each sample point. Note that the sample points occur at each peak and trough of the carrier wave, making the sampling frequency twice the PWM frequency. In actual implementations, the sampling frequency may be reduced by half or more to allow more time for calculations.

For the *B* inverter leg, the inverse of the v'_α reference is used. As can be seen in the resulting $v_{A\text{-}B}$ PWM output, PWM components at the PWM carrier frequency cancel out, resulting in an output PWM pulse frequency of twice the carrier frequency.

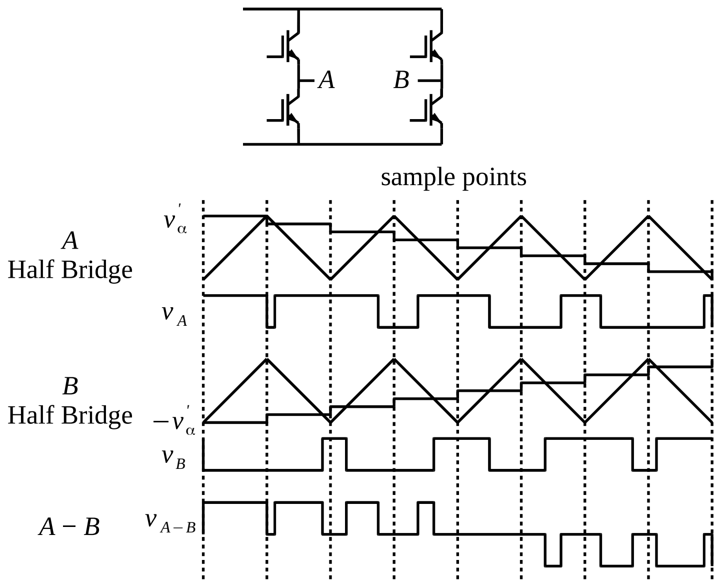

Figure 3.4. Method of generating the 2-phase PWM outputs for the α phase.

The PWM generation process in Figure 3.4 assumes the triangle carrier waveform swings from $+V_{DC}$ to $-V_{DC}$, where V_{DC} is the inverter DC voltage. In reality, the carrier is generated in the pulse width modulator hardware and consists of a counter which counts up from zero to a value depending on the PWM frequency and the clock frequency, then back down to zero. This requires the v'_α reference waveform to be scaled and offset to match the hardware PWM carrier.

The PWM generation process for a 3-phase motor consists of first converting the 2-phase voltage signals v'_α and v'_β to the 3-phase voltage signals v'_u, v'_v and v'_w as described in Chapter 2. These voltage signals can then be re-centred by adding a neutral point modulation waveform to minimise the overall peak-to-peak range to get the maximum output line-to-line voltage swings from the inverter for a given DC supply voltage. This process is shown in Figure 3.5, and the associated waveforms are shown in Figure 3.6. Here, the neutral point modulation waveform chosen is the average of the maximum and minimum values of v'_u, v'_v and v'_w . This is selected because it is easy to generate. A better choice would be the third harmonic sine wave with suitably adjusted waveform amplitude but this is considerably harder to generate so is not used here.

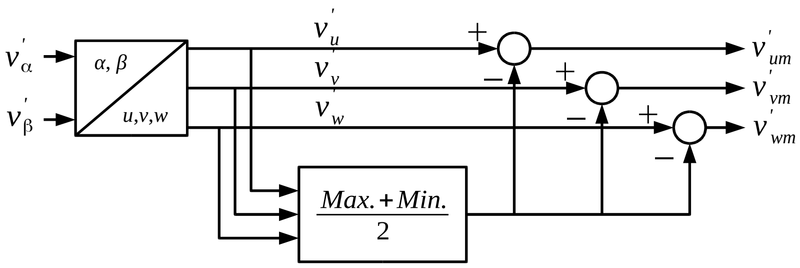

Figure 3.5. Method of centring the PWM inputs for a 3-phase output.

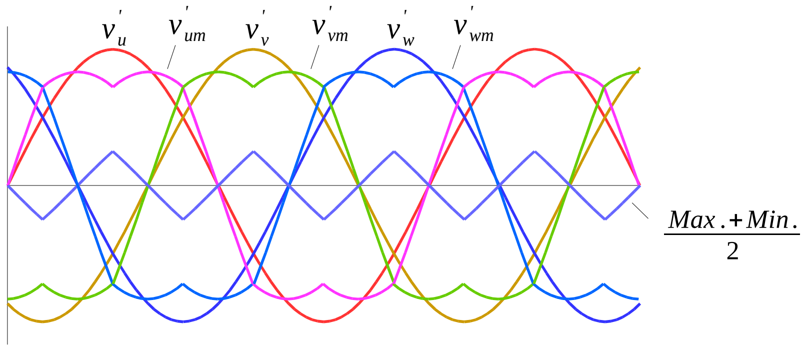

Figure 3.6. PWM centring waveforms.

The resulting three waveforms obtained from the centring process are converted to pulse patterns for each of the three inverter legs using the same method as in Figure 3.4, but using three in-phase carrier waveforms.

Dead Band Compensation

To prevent the likelihood of simultaneous conduction of both the upper and lower transistors in an inverter leg, the PWM hardware delays the turn-on of each transistor by a dead-band delay time. This delays the turning on of each transistor until the opposite transistor is completely turned off. For MOSFET transistors, the delay time is usually set to around 0.3 microseconds.

An unwanted side effect of this delay is that when the output current from the leg is flowing in the direction so that the transistor turning on is conducting (and not its anti-parallel diode), the pulse width applied by this transistor is shortened by the dead-band delay time. This results in the distortion of the output voltage waveform away from the voltage signal applied to the pulse width modulator. This distortion results in unwanted distortion of the output current waveform.

Another side effect is that the voltage signal no longer matches the output voltage. This is a problem for tuning the controller, which relies on the voltage signal being correct to measure both the motor resistance and the back emf.

To force the actual output voltage of each inverter leg to match the voltage signal, the controller adds a voltage offset signal to the input of the pulse width modulator to compensate for the dead band distortion.

The required offset voltage versus the measured average current level is very non-linear in practice due to the PWM-induced ripple current on the phase outputs. For average output currents below the peak of the ripple current, the transistor in the output phase leg to be turned off is always conducting, so the required offset voltage is zero. There is then a transition period from no compensation to full compensation as the average current increases further.

A diagram of the basic compensation method for the *u* phase is shown in Figure 3.7. This is repeated for the *v* and *w* phases.

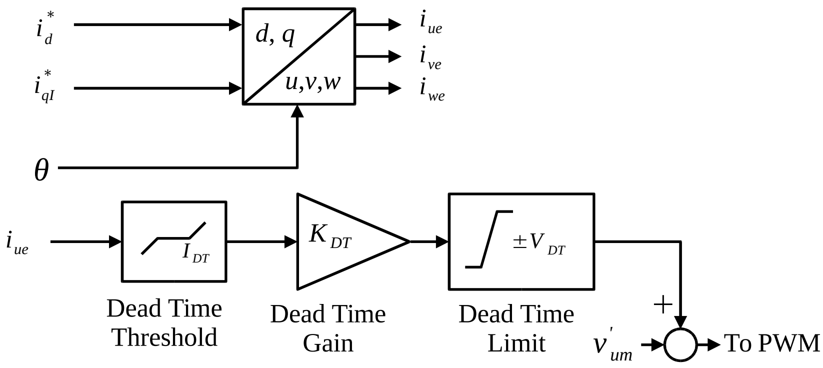

Figure 3.7. Dead band delay time compensation shown for u phase.

The feed forward estimated currents in the rotating *d* and *q* coordinates, i^*_d (Chapters 1 & 6) and i^*_{qI} (Chapter 5), are converted and rotated back to estimated phase currents i_{ue}, i_{ve} and i_{we}. For each phase, the estimated current is first passed through a threshold dead band then amplified then clipped to the required offset voltage signal before being added to the pulse width modulator input signal.

Note that the dead time correction cannot be incorporated into any of the current feedback adjustment loops because the positive Dead Time Gain would cause instability. Only the unadjusted *d* and *q* coordinate currents can be used to generate the estimated phase currents. The resulting errors in dead time estimates due to this restriction have been found to have little effect on overall controller performance.

The dead time threshold current I_{DT}, below which no dead time compensation voltage is applied, is set to an estimate of the amplitude of the ripple current. The actual formula used is:

$$I_{DT}=\frac{T}{L}\left[\frac{rpm}{Kv}\left(1-\frac{rpm}{Kv.V_{DC}}\right)\right]$$

where T is one-half the PWM period, rpm is the speed in rpm, Kv is the Kv motor constant in rpm/Volt, and V_{DC} is the supply voltage.

The formula calculates the motor emf times the PWM off time divided by the inductance to obtain the change in current during the off time. The inner bracket expression is an estimate of the average PWM off-time duty cycle.

The required dead time gain K_{DT} is dependant on the proportion of the dead band period when no current flows versus the average current, which in turn depends on the rate of change of current in the dead band period. This rate of change of current depends on the supply voltage and the inductance and can be estimated.

The dead time limit V_{DT} is set by the pulse width modulator dead time delay setting, but the dead time gain K_{DT} must be adjusted by trial and error, usually to minimise current waveform distortion.

For this motor controller, dead time compensation is not required for good performance, but it is needed for tuning measurements and to reduce losses from output current distortion.

Dead Band Instability

There is another effect from insertion of the dead band which impacts low speed performance. When the rate of change of current is such that it reaches zero during the dead band period, output voltage is controlled by the current level and not by the pulse width. This requires the d-axis stabilising current to be kept on to a higher speed than would otherwise be needed to prevent the controller going unstable. More details can be found in Chapter 4: Rotor Position Error Calculator.

References

[1] Y. Iwaji, T. Sukegawa, T. Okuyama, T. Ikimi, M. Shigyo and M. Tobise. "A new PWM method to reduce beat phenomenon in large-capacity inverters with low switching frequency," IEEE Trans. Ind. Appl., vol. 35, no. 3, pp. 606-612, May/June 1999.

[2] G. P. Hunter, “Low cost cycloconverter induction motor drives using new modulation techniques,” Ph.D. thesis, Fac. Eng & I.T., Univ. Tech. Syd., Sydney, Australia, 1997.